

## Observation of Orientation Propensity for Electron Capture in Multiply-Charged-Ion-Atom Collisions

P. Roncin, C. Adjouri, M. N. Gaboriaud, L. Guillemot, and M. Barat

*Laboratoire des Collisions Atomiques et Moléculaires, Bâtiment 351, Université Paris-Sud, F-91405 Orsay CEDEX, France*

N. Andersen

*Physics Laboratory, H. C. Ørsted Institute, DK-2100 Copenhagen, Denmark*

(Received 3 August 1990)

We have measured the circular polarization of photons emitted after electron capture into the  $B^{2+}(1s^2 2p)$  state in  $B^{3+}(1s^2)+He(1s^2)$  collisions in a planar scattering experiment, using the polarized-photon-scattered-ion coincidence technique. The energy is 1.5–12 keV and scattering angles  $\theta$  are less than  $1.5^\circ$ . For large impact parameters a *strong propensity for orientation* is observed, with the sense of electron orbiting in the *same* direction as the rotation of the internuclear axis being favored by more than a factor of 2 compared to the opposite orientation. This is in qualitative agreement with recent theoretical predictions.

PACS numbers: 34.70.+e

Orientation in inelastic collisions, i.e., a preferential sense of rotation of the active electron around the atomic core in a planar scattering geometry, was first investigated for *excitation* processes by electron impact.<sup>1</sup> Earlier discussions of this problem for ion impact can be found in the review by Hertel *et al.*<sup>2</sup> For keV heavy-particle collisions simple propensity rules for orientation in direct excitation were proposed<sup>3</sup> and later confirmed and generalized in several experimental and theoretical investigations.<sup>4</sup> At low energy, Russek, Kimball, and Cavagnero<sup>5</sup> tackle this subject in the quasimolecular regime for a curve-crossing phenomenon.

The problem of orientation effects in *charge transfer* is more intricate since the active electron changes center. It was first speculated on in connection with the interpretation of Rydberg states in  $H^+-H$  collisions<sup>6</sup> and discussed in terms of velocity matching and of the orientation of the plane of the electron orbit with respect to the incident beam direction. This triggered interest in pursuing the problem to see whether these ideas could be pushed further. For example, for an electron circulating in the collision plane, does the relative momentum of the active electron and the incoming ion influence the electron capture probability? If yes, this should give a difference between capture on the right-hand and left-hand sides of an oriented atom. Resonant charge-transfer collisions were first studied in  $Na^+-Na(3p)$  collisions and showed a small but distinct orientation at large impact parameters at 50–100 eV.<sup>7</sup> At larger velocity, this question was addressed theoretically by Dubois, Hansen, and Nielsen<sup>8</sup> and Allan *et al.*<sup>9</sup> for near-resonant charge exchange in  $H^+-Na(3p)$  collisions in connection with experimental work by Doweck *et al.*<sup>10</sup>

We selected, in the time-reversed scheme, a system consisting of a multiply charged ion and a rare gas because here charge transfer is known to occur near a well-defined curve crossing. These systems offer at the

same time the possibility of studying the large-impact-parameter behavior at reasonably large scattering angles because of the long-range Coulombic repulsion. The  $B^{3+}(1s^2)-He(1s^2)$  system was chosen for the following reasons.

(i) Only two capture channels, leading to  $B^{2+}(1s^2 2s)$  and  $B^{2+}(1s^2 2p)$ , are effective, since higher-lying capture states as well as two-electron capture channels are endothermic by several eV; see Fig. 1. Furthermore, the two curve crossings are located at distances where capture occurs with high probability.

(ii) The B III  $2^2S-2^2P$  transition has a wavelength at 207 nm. Here photomultipliers have high quantum efficiency, vacuum spectrometry is not required, and polarization analysis is possible with high efficiency.

(iii) The capture process leaves the  $He^+(1s)$  target in a single atomic state. Full coherence of the emitted light is then expected (neglecting for the moment post-collisional fine and hyperfine structure effects), contrary to the case of all other rare-gas targets.

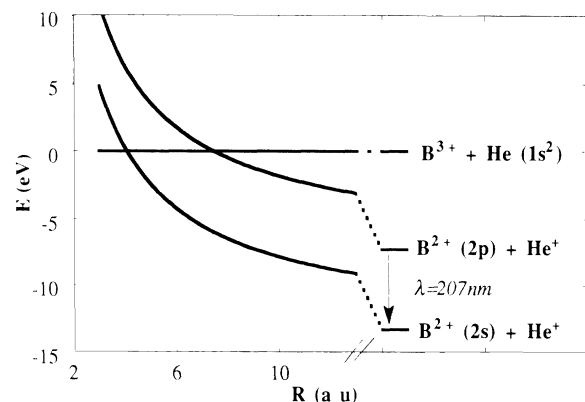


FIG. 1. Schematic potential-energy curves for the most important  $B^{3+}-He$  channels.

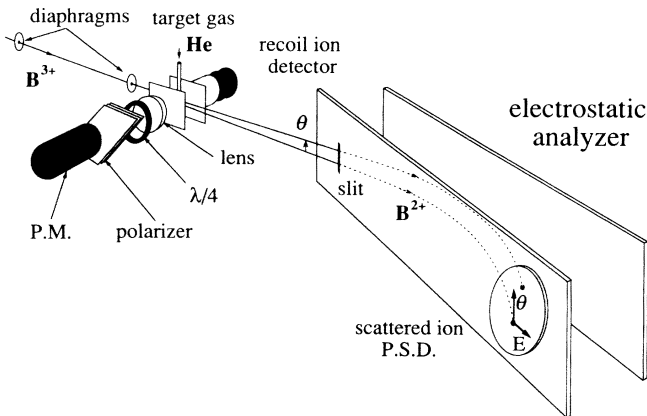


FIG. 2. A diagram of the experimental setup. For discussion see text.

A recent theoretical analysis of this system has been carried out by Hansen *et al.*,<sup>11</sup> and a strong orientation propensity was predicted. This paper reports the first experimental investigation of orientation produced in collisions involving multiply charged ions, i.e., the population dependence on the magnetic quantum number  $m$ . Previously, total and differential cross sections have been determined only as a function of principal quantum number  $n$  and orbital quantum number  $l$ .

The experimental setup is shown schematically in Fig. 2. It has been described in detail elsewhere<sup>12</sup> except for the photon detection and analysis system. Briefly, a mass-selected  $B^{3+}$  beam of energy 1.5–12 keV is produced by the ECR ion source available at the LAGRIP-PA facility in Grenoble. The ion beam crosses an effusive He target beam at a right angle. Scattered ions enter a parallel-plate electrostatic analyzer through a vertical slit and are detected by a position-sensitive detector (PSD) made of two microchannel plates. The position in the horizontal direction gives the energy  $E$  and the charge state of the projectile, and the vertical position gives the scattering angle  $\theta$ , as indicated. Recoil ions are extracted by a weak electric field in order not to perturb the scattered beam and then accelerated onto another channel-plate detector. The time-of-flight difference between scattered and recoil ions allows identification of the charge state of the recoil ions.

For this particular experiment a photon detection system has been added, facing the recoil-ion detector. It consists of first a light-collecting lens of solid angle  $\epsilon=4\%$  having the focal point close to the collision center. An identical subsequent lens focuses the light on a UV photomultiplier (Hamamatsu R2078). Inserted between the two lenses are a  $\lambda/4$  plate for circular polarization analysis and a pile-of-plates Brewster-angle linear polarizer with nine Tetrasil B plates of 1-mm thickness. The transmission of the linear polarizer has been measured at 207 nm using the synchrotron-radiation source available at Laboratoire pour l'Utilisation du Rayonnement Elec-

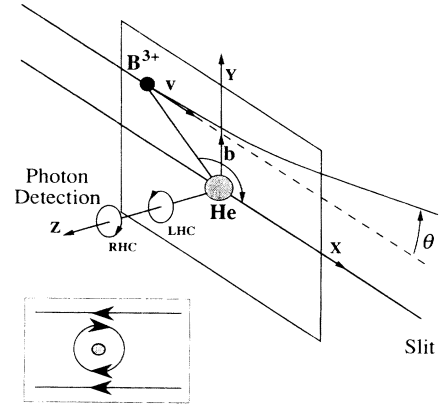


FIG. 3. The standard collision geometry used in the present experiment. Inset: The geometry of the velocity-matching condition of the time-reversed process shown schematically.

tromagnetique (LURE) and found to be 96% and 9.8% in the two main directions, respectively.

Photons and/or recoil ions can be measured in coincidence with the scattered particles using a multicoincidence technique.<sup>12</sup> All particles, recoil ions, scattered ions, and photons, are recorded simultaneously in coincidence. In this work two types of data will be presented: (i) recoil-ion-scattered-ion coincidences which allow simultaneous determination of the differential cross sections for the two capture channels, and (ii) polarized-photon-scattered-ion coincidences which allow separation of the contributions leading to right-hand (RHC) and left-hand (LHC) circularly polarized photons. The numbers of LHC and RHC photons directly reflect the populations of the  $B^{2+}(2p) m = \pm 1$  states, respectively, where the magnetic quantum number  $m$  refers to a quantization axis perpendicular to the collision plane; see Fig. 3. The  $m=0$  state is not populated for symmetry reasons, the fine structure does not reduce the circular polarization, and hyperfine-structure effects can be neglected in this case.<sup>13</sup>

The recoil-ion-scattered-ion coincidences are also used to compensate for possible long-term beam-current and gas-pressure variations.

Figure 4(a) shows energy-gain and angle-resolved spectra at 1.8-keV energy for  $B^{2+}$  scattered ions detected in coincidence with  $He^+$  recoil ions. The dominant structure is due to  $B^{2+}(2s)$  ground-state capture and the secondary peak corresponds to capture into the  $B^{2+}(2p)$  state. From these angular-symmetric raw data, the corresponding differential cross sections  $d\sigma/d\Omega$  are displayed in Fig. 4(b). Stueckelberg oscillations are clearly visible in the angular pattern and are displayed here as sensitive tests of future scattering calculations. From these data we derive a total cross-section ratio  $\sigma(2s):\sigma(2p) = 1.6 \pm 0.2$  which compares well with the energy-gain spectra of Matsumoto *et al.*<sup>14</sup> Unfortunately,

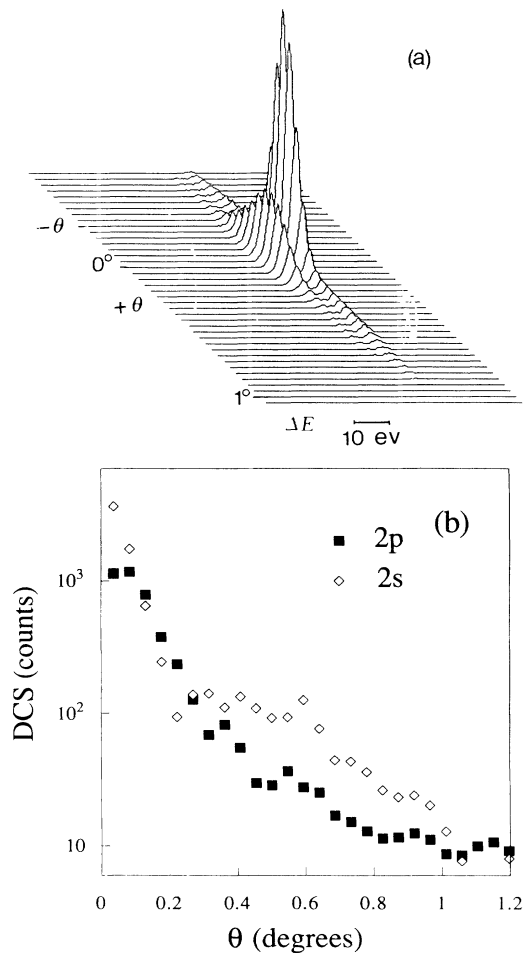


FIG. 4. (a) Doubly differential ( $\theta, \Delta E$ ) spectra of the scattered  $B^{2+}$  ions at 1.8-keV impact energy. (b) Corresponding differential cross sections for electron capture into the  $B^{2+}(2s)$  and  $B^{2+}(2p)$  states.

ly, total and differential cross sections were not evaluated by Hansen *et al.*<sup>11</sup>

Proceeding now to analysis of right-left scattering asymmetry, Fig. 5(a) shows the angular profile of scattered ions in coincidence with RHC and LHC photons. Despite an incident-beam angular spread of about  $0.08^\circ$  a strong right-left asymmetry is observed. Referring to the standard geometry of Fig. 3 there is thus a strong propensity for population of the  $m = -1$  state, in qualitative agreement with the theoretical prediction of Hansen *et al.*<sup>11</sup> A quantitative comparison will have to await evaluation of theoretical angular scattering profiles. Figure 5(b) shows the circular polarization revealing an orientation propensity of at least 2:1 at small scattering angles. This propensity holds at least until 12 keV, the highest energy investigated. The propensity decreases and even reverses at larger scattering angles, i.e., smaller impact parameters, also in agreement with theory.<sup>11</sup> Within our statistics, limited at large scattering angles,

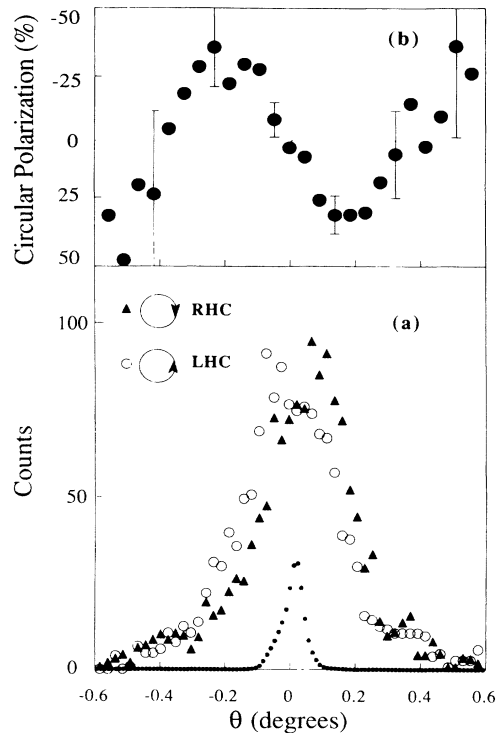


FIG. 5. (a) Scattering profiles of 1.5-keV  $B^{2+}(2p)$  ions in coincidence with RHC and LHC polarized photons for the geometry of Fig. 3. The small circles indicate the incident- $B^{3+}$ -beam angular profile with  $\text{FWHM} = 0.08^\circ$ . (b) Circular polarization  $(\text{RHC} - \text{LHC})/(\text{RHC} + \text{LHC})$  vs scattering angle.

this tendency is found also at other energies.

Similar results have been obtained with a Ne target for which most of the capture populates the  $B^{2+}(2p)$  state. Also for this target the same propensity for  $m = -1$  population is observed at several energies.

In conclusion, we have measured for the first time a differential  $m$  distribution in multiply-charged-ion-atom collisions. A strong propensity for  $m = -1$  population (Fig. 5) has been observed for capture into  $B^{2+}(2p)$  in  $B^{3+}$ -He collisions, thereby extending the validity of propensity rules for orientation in atomic collisions into a new range. Data for a Ne target suggest that the propensity rule may have a wider area of applicability. The present *strong* orientation effect fits the naive picture of "velocity matching,"<sup>15</sup> namely, that electron capture is favored when electron and projectile travel in the same sense of direction; cf. the inset in Fig. 3. When large impact parameters are concerned, the actual velocity to consider is smaller than the average velocity of the  $1s_{\text{He}}$  orbital (1.2 a.u.). This might explain why the effect is so large at our low collision velocity of 0.07 a.u. Future work should concentrate on experimental determination of a complete set of scattering parameters including also the alignment angle, and theoretical evaluation of results differential in scattering angle.

We are grateful to M. Vincent and J. Gallay of LURE and thank LAGRIPPA for providing us with the  $B^{3+}$  beam. Travel support by Institut Français (Copenhagen) was instrumental during preparation of the project. The research was carried out within the frame of the Committee for the European Development of Science and Technology program.

---

<sup>1</sup>M. Kohmoto and U. Fano, *J. Phys. B* **14**, L447 (1981); see also N. Andersen, J. W. Gallagher, and I. V. Hertel, *Phys. Rep.* **165**, 1 (1988).

<sup>2</sup>I. V. Hertel, H. Schmidt, A. Bähring, and E. Meyer, *Rep. Prog. Phys.* **48**, 375 (1985).

<sup>3</sup>N. Andersen and S. E. Nielsen, *Europhys. Lett.* **1**, 15 (1986).

<sup>4</sup>N. Andersen, T. Andersen, P. Dalby, and T. Royer, *Z. Phys. D* **9**, 315 (1988), and references therein.

<sup>5</sup>A. Russek, D. B. Kimball, and M. J. Cavagnero, *Phys. Rev. A* **23**, 139 (1981).

<sup>6</sup>G. A. Kohring, A. E. Wetmore, and R. Olson, *Phys. Rev. A* **28**, 2526 (1983).

<sup>7</sup>R. Witte, E. E. B. Campbell, C. Richter, H. Schmidt, and I. V. Hertel, *Z. Phys. D* **5**, 101 (1987).

<sup>8</sup>A. Dubois, J. P. Hansen, and S. E. Nielsen, *J. Phys. B* **22**, L279 (1989).

<sup>9</sup>R. J. Allan, C. Courbin, P. Salas, and P. Wahnou, *J. Phys. B* (to be published).

<sup>10</sup>D. Doweck, J. C. Houver, J. Pommier, C. Richter, T. Royer, N. Andersen, and B. Palsdottir, *Phys. Rev. Lett.* **64**, 1713 (1990); D. Doweck *et al.* (to be published).

<sup>11</sup>J. P. Hansen, L. Kocbach, A. Dubois, and S. E. Nielsen, *Phys. Rev. Lett.* **64**, 2491 (1990).

<sup>12</sup>M. Barat, M. N. Gaboriaud, L. Guillemot, P. Roncin, H. Laurent, and S. Andriamonge, *J. Phys. B* **20**, 5771 (1987).

<sup>13</sup>Andersen, Gallagher, and Hertel (Ref. 1).

<sup>14</sup>A. Matsumoto, T. Iwai, Y. Kaneko, M. Kimura, N. Kobayashi, S. Ohtani, K. Okuno, S. Takagi, H. Tawara, and S. Tsurubuchi, *J. Phys. Soc. Jpn.* **52**, 3291 (1983).

<sup>15</sup>Notice that propensity rules for excitation of Ref. 3 and that deduced from the analysis of Ref. 5 predict the *opposite* sense of orientation than the one observed here.

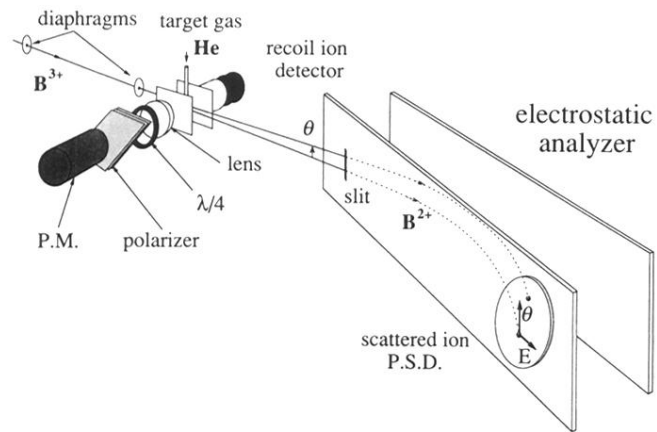


FIG. 2. A diagram of the experimental setup. For discussion see text.

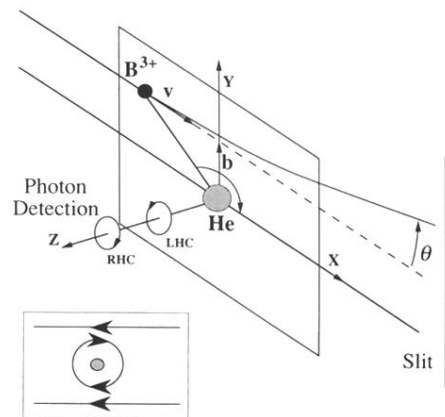


FIG. 3. The standard collision geometry used in the present experiment. Inset: The geometry of the velocity-matching condition of the time-reversed process shown schematically.